Poonam Sangwan

PLANE WAVE PROPAGATION IN EXPONENTIALLY GRADED NONLOCAL COUPLE STRESS SOLID MEDIA UNDER INITIAL STRESS

PROSTIRANJE RAVANSKOG TALASA U ČVRSTOJ SREDINI POD DEJSTVOM INICIJALNOG NAPONA SA EKSPONENCIJALNO GRADIJENTNIM NELOKALNIM VEZANIM NAPONOM

Originalni naučni rad / Original scientific paper
Rad primljen / Paper received: 16.07.2024
https://doi.org/10.69644/ivk-2025-siA-0003

Adresa autora / Author's address:
Department of Mathematics, Chandigarh University, Gharuan, Mohali, India email: poonamsangwan2793@gmail.com

Keywords
- initial stress
- nonlocal
- micropolar
- wave propagation
- functionally graded

Ključne reči
- inicijalni napon
- nelokalni
- mikropolarni
- prostiranje talasa
- funkcionalni gradijentni

Abstract

The study investigates wave propagation in functionally graded nonlocal micropolar elastic media under initial stress. It is found that there are two waves, namely quasi-P and quasi-SV waves. The reflection and refraction coefficients are calculated numerically in form of matrix. Numerical results are carried out to illustrate the reflection and reflection waves against angle of incidence with the help of MATLAB® graphical routines for different values of initial stress parameter. It is observed that derived equations for quasi-P and quasi-SV waves are affected by nonlocal, gradient and initial stress parameters.

Izvod

U radu se proučava prostiranje talasa u funkcionalnoj gradijentnoj nelokalnoj mikropolarnoj elastičnoj sredini pod dejstvom inicijalnog napona. Pokazuje se da postoje dva talasa, zapravo kvazi-P i kvazi-SV talasi. Koeficijenti refleksije i refrakcije se određuju numerički u obliku matrice. Numerički rezultati ilustruju refleksiju i refrakciju talasa pod upadnim uglom, pomoću grafičkih rutina MATLAB® za različite vrednosti parametra inicijalnog napona. Pokazuje se da na izvedene jednačine za kvazi-P i kvazi-SV talase utiču nelokalni, gradijentni i parametri inicijalnog napona.

INTRODUCTION

Voigt /1/ introduced the concept of couple stress. The nonlinear theory of asymmetric elasticity with couple stresses was developed by Cosserat and Cosserat /2/. Later, various Cosserat's type theories were developed by many authors like Toupin /3/, Mindlin and Tiersten /4/, Anthoine /5/, Lubarda and Markenscoff /6/, and Lubarda /7/, etc. Gourgiotis and Georgiadis /8/ presented the technique for studying crack problem within couple stress elastic theory. Güven /9/ studied the influence of modified couple stress theory on nonlocal longitudinal waves. The micropolar theory of elasticity is the extension of classical theory of elasticity investigated by Eringen /10/. The translational degree of freedom with the addition of rotational degree of freedom at the typical material point of the body is considered in this micropolar theory. He assumed three mutually perpendicular rigid directors at the centre of mass of the particles. Wave propagation in couple stress micropolar thermoviscous elastic solid half spaces are discussed by Sahrawat et al. /11/. Poonam et al. /12/ investigated the void and nonlocal parameter had a great effect on fundamental solution in a nonlocal couple stress micropolar thermoelastic solid with voids. Sahrawat et al. /13/ studied the wave propagation in nonlocal couple stress micropolar thermoelastic solid.

Any medium is said to be functionally graded when any property of the medium changes according to a defined function and in defined direction. The functionally graded isotropic medium plays a significant role in the analysis of seismic wave propagation. In this paper, the density and inertia of the material changes exponentially along with other initial stress parameters. Initial stresses are stresses already present in the structure not subjected to the action of external forces. Biot /14/ investigated the impact of initial stress on the waves. Recently, the problems based on the influence of initial stress parameter on the wave propagation with their reflection and refraction phenomenon in functionally graded isotropic medium is discussed by several authors like Tochhawng and Singh /15/, Saha et al. /16/, Goyal and Kumar /17/, Poonam et al. /18/, Wang et al. /19/, and Poonam et al. /20/.

In this paper, we study the wave propagation in functionally graded nonlocal micropolar elastic media under initial stress. We have found that there are two waves, namely quasi-P and quasi-SV waves. The reflection and refraction coefficients are calculated numerically in form of matrix. The numerical results are carried out to illustrate the reflection and refraction waves against angle of incidence with the help of MATLAB® graphical routines for different values of initial stress parameter. It is observed that the derived equations for quasi-P and quasi-SV waves is affected by nonlocal, gradient, and initial stress parameters.

MATHEMATICAL FORMULATION AND GEOMETRY

The plane interface coincides with x_2x_3-plane in the coordinate system $0x_1x_2x_3$ and x_3 axis taking along the interface $x_2 = 0$. We consider two regions H_1 and H_2 occupying $x_2 \geq 0$ and $x_2 \leq 0$, respectively, as shown in Fig. 1.

Following Mindlin and Tiersten /4/, and Biot /14/, the stress-strain relation including hydrostatic pressure h is given

$$(1-\varepsilon^2\nabla^2)t_{22}=(\lambda+2\mu+h)\frac{\partial u_2}{\partial x_2}+(\lambda+h)\left(\frac{\partial u_1}{\partial x_1}+\frac{\partial u_3}{\partial x_3}\right), \quad (1)$$

$$(1-\varepsilon^2\nabla^2)t_{33}=(\lambda+2\mu+h)\frac{\partial u_3}{\partial x_3}+(\lambda+h)\left(\frac{\partial u_2}{\partial x_2}+\frac{\partial u_1}{\partial x_1}\right), \quad (2)$$

$$(1-\varepsilon^2\nabla^2)t_{23}=\mu\left(\frac{\partial u_2}{\partial x_2}+\frac{\partial u_3}{\partial x_3}\right)-a\left\{\frac{\partial}{\partial x_2}\left(\frac{\partial^2 u_3}{\partial x_2^2}+\frac{\partial^2 u_3}{\partial x_3^2}\right)-\right.$$
$$\left.-\frac{\partial}{\partial x_3}\left(\frac{\partial^2 u_2}{\partial x_2^2}+\frac{\partial^2 u_2}{\partial x_3^2}\right)\right\}. \quad (3)$$

FUNCTIONALLY GRADED COUPLE STRESS THERMO-ELASTIC MEDIUM h_s (s = 1, 2)

The material constants $a^{(s)}$, $\mu^{(s)}$, $\lambda^{(s)}$, ρ_s and h_s (s = 1, 2) of functionally graded media in the exponential form w.r.t. depth are submitted as

$\mu^{(1)}=\underline{\mu}e^{\beta_1 x_2}$, $\mu^{(2)}=\underline{\mu}e^{\beta_2 x_2}$, $\lambda^{(1)}=\underline{\lambda}e^{\beta_1 x_2}$, $\lambda^{(2)}=\underline{\lambda}e^{\beta_2 x_2}$,
$a^{(1)}=\underline{a}e^{\beta_1 x_2}$, $a^{(2)}=\underline{a}e^{\beta_2 x_2}$, $\rho_s=\rho^{(s)}e^{\beta_s x_2}$, $h_s=h^{(s)}e^{\beta_s x_2}$,

where: $\underline{a}$, μ, $\underline{\lambda}$ are constitutive coefficients w.r.t. h_1 and h_2, respectively. $\rho^{(s)}$, $h^{(s)}$ and β_s are density, pressure and gradient parameter, respectively.

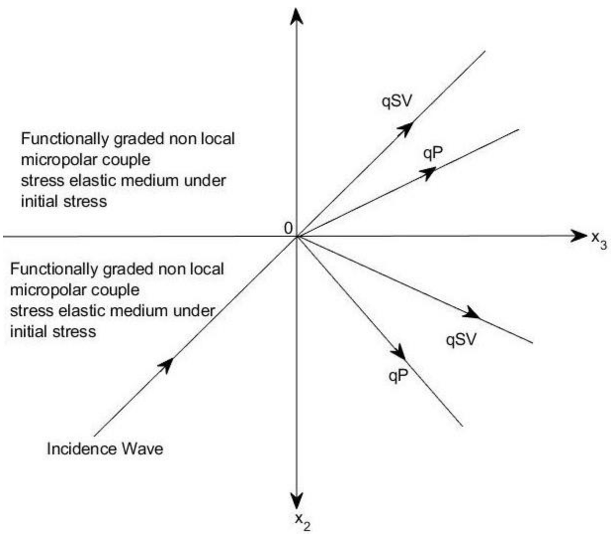

Figure1. Geometry of the problem.

MEDIUMS h_s UNDER INITIAL STRESSES

Let the initial stresses along x_2 and x_3 axes be $I_{22}^{(s)}$ and $I_{22}^{(s)}$, respectively for both mediums, with the functionally gradient property in the form of exponent,

$$I_{22}^{(s)}=I_{22}^{(0s)}e^{\beta_s x_2},\ I_{33}^{(s)}=I_{33}^{(0s)}e^{\beta_s x_2}, \quad (5)$$

where: $I_{22}^{(s)}$ and $I_{22}^{(s)}$ admit $I_{22}^{(0s)}$ and $I_{22}^{(0s)}$ at the common interface.

Following Biot /14/ and using Eqs. (5) and (1)-(3), the equations of motion are

$$\frac{\partial t_{22}}{\partial x_2}+\frac{\partial t_{23}}{\partial x_3}-I^{(1)}\frac{\partial\omega_{32}}{\partial x_3}=\rho_1\frac{\partial^2 u_2}{\partial t^2}, \quad (6)$$

$$\frac{\partial t_{23}}{\partial x_2}+\frac{\partial t_{33}}{\partial x_3}-I^{(1)}\frac{\partial\omega_{32}}{\partial x_2}=\rho_1\frac{\partial^2 u_3}{\partial t^2}, \quad (7)$$

where: $I^{(1)} = I_{33}^{(1)} - I_{22}^{(1)}$ and $\omega_{32}=\frac{1}{2}\left(\frac{\partial u_3}{\partial x_2}+\frac{\partial u_2}{\partial x_3}\right)$.

Using Eq.(5), we obtain $I^{(1)} = S^{(1)}e^{\beta 1x2}$ with $S^{(1)} = I_{22}^{(1)} - I_{33}^{(1)}$. Also, for initial stresses of medium h_2 we can use subscript '2' in place of '1'.

According to the Helmholtz decomposition theorem on vectors, we introduce displacement potentials σ and Σ as

$$u=\nabla\sigma+\nabla\times\Sigma,\ \nabla\cdot\Sigma=0. \quad (8)$$

Using Eq.(8) in Eqs.(6)-(7), we obtain

$$(\underline{\lambda}+2\underline{\mu}+\underline{h})\nabla^2\sigma=\rho_1\frac{\partial^2\sigma}{\partial t^2}, \quad (9)$$

$$\underline{a}\nabla^2\nabla^2\Sigma+S^{(1)}\nabla^2\Sigma=\rho_1\frac{\partial^2\Sigma}{\partial t^2}. \quad (10)$$

We assume the solution for wave propagation of the form

$$\{\sigma,\Sigma\}=(a,\mathbf{A})\exp\{il(\mathbf{n}.\mathbf{r}-ct)\}, \quad (11)$$

where: let $\omega = cl$ is frequency; c is phase velocity; and l is wave number; a and $\mathbf{A}$ are scalar and vector amplitudes; coordinate $\mathbf{r} = xm$ (m = 2, 3); $\mathbf{n}$ is the unit vector.

Using Eq.(11) in Eq.(9), we obtain

$$S_1^2=\left[\frac{(\lambda^{(1)}+\mu^{(1)}+K^{(1)})}{\rho^{(1)}}-\varepsilon^2\omega^2\right]. \quad (12)$$

Using Eq.(11) in Eq.(10), we obtain

$$\rho_1 S^4-I^{(1)}S^2+\underline{a}\omega^2=0.$$

The solution of the above equation can be written as

$$S_2^2=\frac{I^{(1)}\pm\sqrt{{I^{(1)}}^2-4\underline{a}\rho_1\omega^2}}{2\rho_1}. \quad (13)$$

Here, the speeds S_1 and S_2 are corresponding to the qP and qSV -wave, respectively. Thus, we find two waves, namely, quasi-shear (qSV)-wave and quasi-P(qP) waves.

Reflection-refraction phenomenon

Let us consider that waves are incident at the $x_2 = 0$, by making an angle θ_0. The incident waves will generate three reflected waves and three refracted waves by making angles θ_s and θ_s' with speeds S_s and S_s' for h_1 and h_2, respectively, where s = 1, 2.

The values for speeds S_s' are same as for S_s, respectively, with the primes at the significant places and replacing ρ_1 by ρ_2.

Boundary conditions: the boundary conditions for media h_1 and h_2 are given by

$$u_2=u_2',\ u_3=u_3',\ m_{21}=m_{21}',\ t_{23}=t_{23}',\ t_{22}=t_{22}'. \quad (14)$$

For incident qP-waves:

When qP-wave is incident, then the angles θ_s, θ_s' and the wave numbers l_s, l_s' (s = 1, 2) are connected by the relations

$$l_1\sin\sin\theta_1 = l_2\sin\sin\theta_2 = l_1'\sin\sin\theta_1' = l_2'\sin\sin\theta_2'.$$

The values of σ and Σ for medium h_1 is given by

$$\sigma=M_0\exp\{il_1(x_2\sin\theta_0-x_3\cos\theta_0)-i\omega t\}+$$
$$+M_1\exp\{il_1(x_2\sin\theta_1-x_3\cos\theta_1)-i\omega t\}, \quad (15)$$

$$\Sigma=M_2\exp\{il_2(x_2\sin\sin\theta_2-x_3\cos\cos\theta_2)-i\omega t\}. \quad (16)$$

The values of σ', and Σ' for medium h_2 is given by

$$\sigma'=M_1'\exp\{il_1'(x_2\sin\sin\theta_1'-x_3\cos\cos\theta_1')-i\omega' t\}, \quad (17)$$

$$\Sigma'=M_2'\exp\{il_2'(x_2\sin\sin\theta_2'-x_3\cos\cos\theta_2')-i\omega' t\}. \quad (18)$$

Using Eq.(14) in Eqs.(15)-(18), we obtain

$$[(\underline{\lambda}+\underline{h})+2\underline{\mu}\theta_0]l_1^2M_0+[(\underline{\lambda}+\underline{h})+2\underline{\mu}\theta_1]l_1^2M_1+$$
$$+2\underline{\mu}M_2l_2^2\sin\theta_2\cos\theta_2-[(\bar{\bar{\lambda}}+\bar{\bar{h}})+2\bar{\bar{\mu}}'l\theta_1']l_1'^2M_1'-$$
$$-2\bar{\bar{\mu}}M_2'l_2'^2\sin\theta_2'\cos\theta_2'=0\,, \qquad (19)$$

$$-\underline{\mu}M_0l_1^2-\underline{\mu}M_1l_1^2-\underline{a}M_2l_2^4+\bar{\bar{\mu}}M_1'l_1'^2+\bar{\bar{a}}M_2'l_2'^4=0\,, \qquad (20)$$

$$M_0\sin 2\theta_0(\sin\theta_0+\cos\theta_0)l_1^3+M_1\sin 2\theta_1(\sin\theta_1+\cos\theta_1)l_1^3-$$
$$-M_2\sin 2\theta_2(\sin\theta_2+\cos\theta_2)l_2^3+M_1'\sin 2\theta_1'(\sin\theta_1'+\cos\theta_1')l_1'^3+$$
$$+M_1'\sin 2\theta_2'(\sin\theta_2'+\cos\theta_2')l_1'^3=0\,, \qquad (21)$$

$$M_0l_1\cos\theta_0+M_1l_1\cos\theta_1-M_2l_2\sin\theta_2-M_1'l_1'\cos\theta_1'+$$
$$+M_2'l_2'\sin\theta_2'=0\,, \qquad (22)$$

$$M_0l_1\sin\theta_0+M_1l_1\sin\theta_1-M_2l_2\cos\theta_2-M_1'l_1'\sin\theta_1'+$$
$$+M_2'l_2'\cos\theta_2'=0\,. \qquad (23)$$

Equations (19)-(23) can be written as

$$[H][Q]=[Z]\,, \qquad (24)$$

where: $[H] = [h_{ij}]$ is a 5×4 matrix; $[Q] = [Q_1, Q_2, Q_3, Q_4]$ is a 4×1 column matrix; $Q_r = M_r/M_0$ (r = 1, 2) and $Q_t = M'_{t\text{-}3}/M_0$ (t = 4, 5) are amplitude ratios. The non-zero entries of the matrices are given in ‘Appendix A’.

For incident qSV-wave:

The values of σ and Σ for medium h_1 are given by

$$\sigma=M_1\exp\exp\{il_1(x_2\sin\sin\theta_1+x_3\cos\cos\theta_1)-i\omega t\}\,, \qquad (25)$$

$$\Sigma=M_0\exp\exp\{il_1(x_2\sin\sin\theta_0+x_3\cos\cos\theta_0)-i\omega t\}+$$
$$+M_2\exp\exp\{il_2(x_2\sin\sin\theta_2+x_3\cos\cos\theta_2)-i\omega t\}\,. \qquad (26)$$

The values of σ' and Σ' for medium h_2 are given by

$$\sigma'=M_1'\exp\exp\{il_1'(x_2\sin\sin\theta_1'+x_3\cos\cos\theta_1')-i\omega' t\}\,, \qquad (27)$$

$$\Sigma'=M_2'\exp\exp\{il_2'(x_2\sin\sin\theta_2'+x_3\cos\cos\theta_2')-i\omega' t\}\,. \qquad (28)$$

Using Eq.(14) in Eqs.(25)-(28), we obtain

$$2\underline{\mu}M_0l_3^2\sin\theta_2\cos\theta_2+[(\underline{\lambda}+\underline{h})+2\underline{\mu}\theta_1]l_1^2M_1+2\underline{\mu}M_2l_2^2\sin\theta_2\times$$
$$\times\cos\theta_2-[(\bar{\bar{\lambda}}+\bar{\bar{h}})+2\bar{\bar{\mu}}'l\theta_1']l_1'^2M_1'-2\bar{\bar{\mu}}M_2'l_2'^2\sin\theta_2'\cos\theta_2'=0, \qquad (29)$$

$$-\underline{a}M_0l_2^4-\underline{\mu}M_1l_1^2-\underline{a}M_2l_2^4+\bar{\bar{\mu}}M_1'l_1'^2+\bar{\bar{a}}M_2'l_2'^4=0\,, \qquad (30)$$

$$M_0\sin 2\theta_0(\sin\theta_0+\cos\theta_0)l_3^3+M_1\sin 2\theta_1(\sin\theta_1+\cos\theta_1)l_1^3-$$
$$-M_2\sin 2\theta_2(\sin\theta_2+\cos\theta_2)l_2^3+M_1'\sin 2\theta_1'(\sin\theta_1'+\cos\theta_1')l_1'^3+$$
$$+M_1'\sin 2\theta_2'(\sin\theta_2'+\cos\theta_2')l_2'^3=0\,, \qquad (31)$$

$$M_0l_3\cos\theta_0+M_1l_1\cos\theta_1-M_2l_2\sin\theta_2-M_1'l_1'\cos\theta_1'+$$
$$+M_2'l_2'\sin\theta_2'=0\,, \qquad (32)$$

$$M_0l_3\sin\theta_0+M_1l_1\sin\theta_1-M_2l_2\cos\theta_2-M_1'l_1'\sin\theta_1'+$$
$$+M_2'l_2'\cos\theta_2'=0\,. \qquad (33)$$

Equations (29)-(33) can be written as

$$[U][V]=[W]\,, \qquad (34)$$

where: $[U] = [U_{ij}]$ is a 5×4 matrix; $[V] = [V_1, V_2, V_3, V_4]$ is a column matrix; $V_r = M_r/M_0$ (r = 1, 2) and $V_t = M'_{t\text{-}3}/M_0$ (t = 4, 5) are amplitude ratios. The non-zero entries in matrices are given in ‘Appendix B’

NUMERICAL ANALYSIS

The influence of initial stress parameter on the reflection and refraction coefficients w.r.t. angle of incidence is drawn graphically by the usage of MATLAB® software. Numerical values for h_1 and h_2 are taken from Tochhwang et al. /15/.

For h_1, the parameters are given by: $\underline{\lambda}$ = 3.071·10^{11} N/m^2, $\underline{\mu}$ = 3.581·10^{11} N/m^2, $\underline{K}$ = 0.690·10^2 W/m°, $\underline{\beta}$ = 7.04·10^6 N/m^2, $\rho^{(1)}$ = 8.836·10^3 kg/m^3, $\underline{a}$ = 1.650·10^{11} N/m^2.

For h_2, the parameters are given by: $\bar{\lambda}$ = 1.628·10^{11} N/m^2, $\bar{\mu}$ = 0.627·10^{11} N/m^2, $\bar{\beta}$ = 5.75·10^{11} N/m^2, $\bar{K}$ = 1.24·10^2 W/m°, $\rho^{(1)}$ = 7.13·10^3 kg/m^3, $\bar{a}$ = 0.362·10^{11} N/m^2.

The gradient parameters are

$$\frac{I^{(1)}}{\mu}=\frac{I^{(2)}}{\mu}=0,\ \pm 4\,.$$

Figures 2-5 and 6-9 illustrate the influence of initial stress for qP- and qSV-waves on reflection and refraction coefficients w.r.t. angle of incidence θ_0. Six curves in the figures represent the following characteristics of initial stress.

Curve 1 gives values where h_1 does not contain initial stress but h_2 contains initial stress.

Curve 2 gives values where compressive initial stress exists in h_1.

Curve 3 gives values where tensile initial stress exists in h_1.

Curve 4 gives values where h_1 contains initial stress but h_2 does not contain initial stress.

Curve 5 gives values where compressive initial stress exists in h_2.

Curve 6 gives values where tensile initial stress exists in h_2.

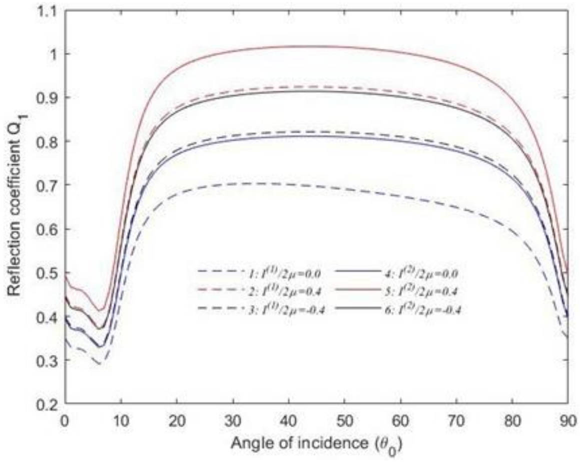

Figure 2. Q_1 vs. θ_0 for qP-wave with the influence of initial stress.

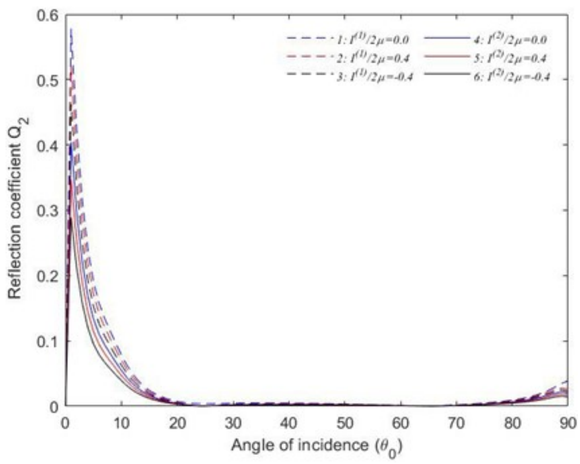

Figure 3. Q_2 vs. θ_0 for qP-wave with the influence of initial stress.

Figures 2-4 describe the effect of $I^{(1)}/2\mu$ and $I^{(2)}/2\mu$ on the reflection and refraction coefficients Q_i (i = 1…6) w.r.t. θ_0.

Figure 2 illustrates that the initial stress parameter for both mediums has a decreasing influence on Q_i for nearly $0° \leq \theta_0 \leq 8°$ and $86° \leq \theta_0 \leq 90°$, but an increasing influence for nearly $8° \leq \theta_0 \leq 85°$. After studying the curves, we observe that curves 5 and 6 support more to Q_i as compared to curves 2 and 3. The influence of curves 2 and 5 on Q_i is more as compared to curves 3 and 6. Curve 1 supports more to Q_i than curve 4.

Figure 3 depicts that the initial stress parameter for both mediums has a decreasing influence on Q_2 for $0° \leq \theta_0 \leq 90°$. After studying the curves we observe that curves 2 and 3 support more to Q_2 as compared to curves 5 and 6. The influence of curves 2 and 5 on Q_2 is more as compared to curves 3 and 6. Curve 4 supports more to Q_2 than compared to curve 1.

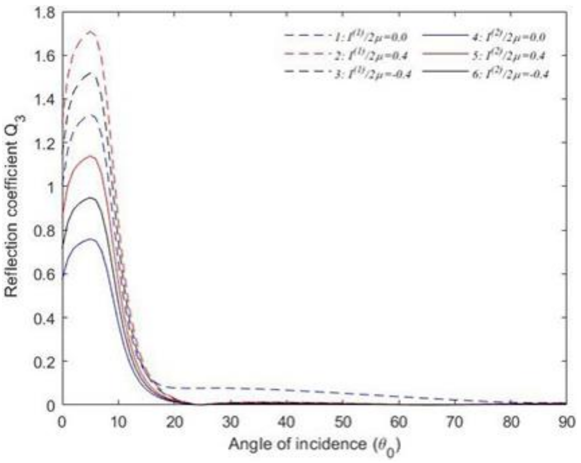

Figure 4. Q_3 vs. θ_0 for qP-wave with the influence of initial stress.

Figure 4 illustrates that the initial stress parameter for both mediums has an increasing influence on Q_3 for nearly $0° \leq \theta_0 \leq 8°$ but decreasing influence for nearly $8° \leq \theta_0 \leq 90°$. After studying, curves 2 and 3 affect more Q_3 as compared to curves 5 and 6. The influence of curves 2 and 5 on Q_3 is more compared to curves 3 and 6. Curve 4 supports more to Q_3 than compared to curve 1.

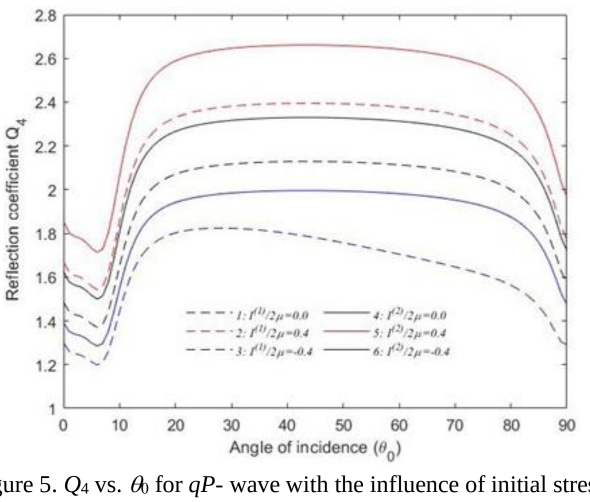

Figure 5. Q_4 vs. θ_0 for qP- wave with the influence of initial stress.

Figure 5 depicts that the initial stress parameter for both mediums has a decreasing influence on Q_4 for nearly $0° \leq \theta_0 \leq 8°$ and $86° \leq \theta_0 \leq 90°$, but an increasing influence for nearly $8° \leq \theta_0 \leq 85°$. After studying the curves we observe that curves 5 and 6 support more to Q_4 as compared to curves 2 and 3. The influence of curves 2 and 5 on Q_4 is more as compared to curves 3 and 6. Curve 1 supports more to Q_4 than compared to curve 4.

Figures 6-9 describe the effect of $I^{(1)}/2\mu$ and $I^{(2)}/2\mu$ on the reflection and refraction coefficients V_i (i = 1…6) w.r.t. θ_0.

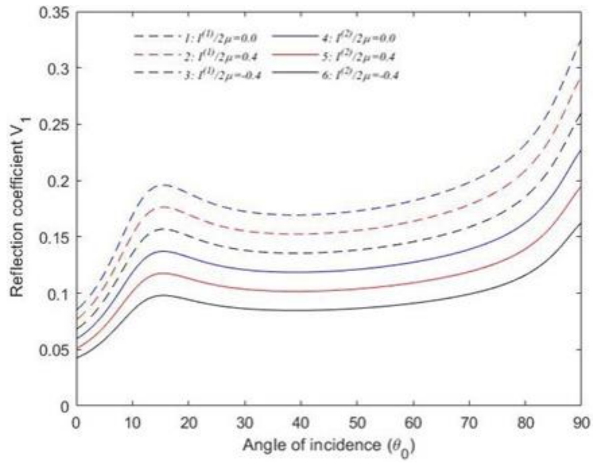

Figure 6. V_1 vs. θ_0 for qSV-wave with the influence of initial stress.

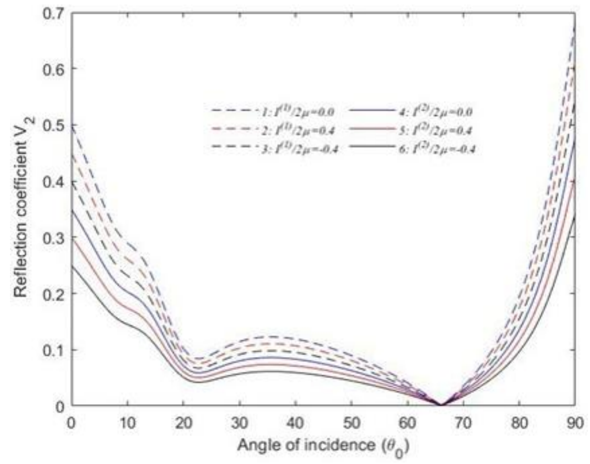

Figure 7. V_2 vs. θ_0 for qSV-wave with the influence of initial stress.

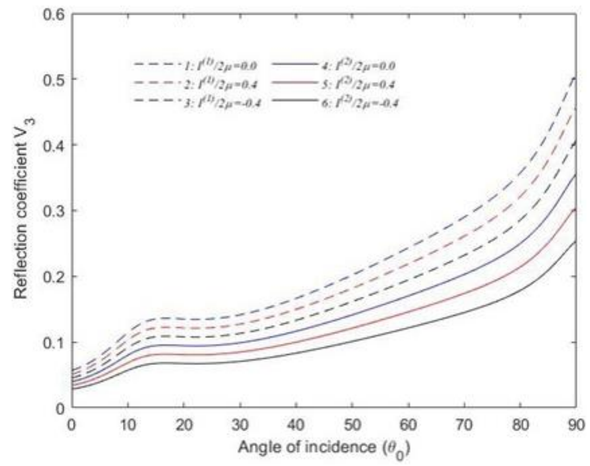

Figure 8. V_3 vs. θ_0 for qSV-wave with influence of initial stress.

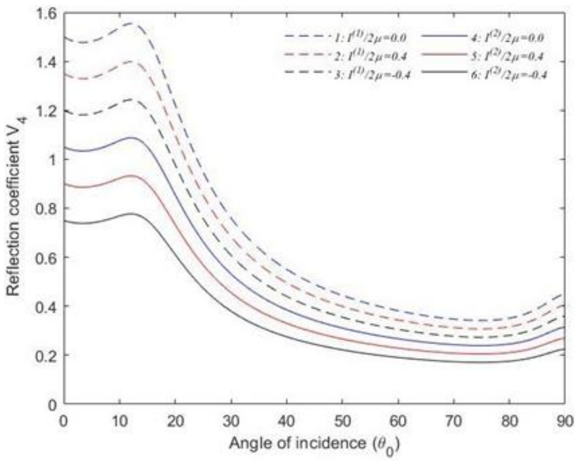

Figure 9. V_4 vs. θ_0 for *qSV*-wave with influence of initial stress.

Figure 6 depicts that the initial stress parameter for both mediums has an increasing influence on V_1 for nearly $0° \leq \theta_0 \leq 15°$ and $40° \leq \theta_0 \leq 90°$ but a decreasing influence for nearly $5° \leq \theta_0 \leq 40°$. Figure 7 illustrates that initial stress parameter for both mediums has an increasing influence on V_2 for nearly $25° \leq \theta_0 \leq 40°$ and $65° \leq \theta_0 \leq 90°$ but a decreasing influence for nearly $0° \leq \theta_0 \leq 20°$ and $40° \leq \theta_0 \leq 65°$. Figure 8 shows that the initial stress parameter for both mediums has an increasing influence on V_3 for $0° \leq \theta_0 \leq 90°$. Figure 9 illustrates that the initial stress parameter for both mediums has a decreasing influence on V_4 for nearly $20° \leq \theta_0 \leq 78°$. After studying the curves we observe that the V_i (i = 1…6) are more significant in h_1 than h_2 under the influence of tensile and initial stress. The compressive initial stress of h_1 and h_2 on V_i (i = 1…6) is more as compared to tensile initial stress of h_1 and h_2. When h_2 contains initial stress but h_1 does not contain initial stress supports more to V_i (i = 1…6) than as compared to the case when h_1 contains initial stress but h_2 does not contain initial stress.

CONCLUSION

We have examined the study of wave propagation due to incidence of quasi-P and quasi-SV waves at the interface of two different functionally graded nonlocal couple stress elastic media under initial stress. Characteristics of plane waves in both mediums are considered mathematically and shown graphically with angle of incidence to study the effects of several parameters.

We have obtained the following conclusions from the given problem:

- the phase speeds, reflection and refraction coefficients for the *qP* and *qSV* waves are considered;
- when *qP*-wave is incident, the influence of tensile and initial stress in h_1 supports more to Q_2 and Q_3 as compared to tensile and compressive initial stress acting in h_2. While the influence of tensile and initial stress in h_2 supports more to Q_1 and Q_4 as compared to tensile and compressive initial stress acting in h_1. But when *qSV*-wave is incident, the influence of tensile and initial stress in h_1 supports more to V_i (i = 1…6) as compared to tensile and compressive initial stress acting in h_2;
- when *qP*-wave is incident, the compressive initial stress of h_1 and h_2 on Q_i (i = 1…6) is more as compared to tensile initial stress of h_1 and h_2. When *qSV*-wave is incident, the compressive initial stress of h_1 and h_2 on V_i (i = 1…6) is more as compared to tensile initial stress of h_1 and h_2;
- when *qP*-wave is incident, the case when h_1 contains initial stress but h_2 does not contain initial stress supports more to Q_2 and Q_3 than as compared to the case when h_2 contains initial stress but h_1 does not contain initial stress, while the case when h_2 contains initial stress but h_1 does not contain initial stress supports more to Q_1 and Q_4 than as compared to the case when h_1 contains initial stress but h_2 does not contain initial stress. When the *qSV*-wave is incident, the case when h_2 contains initial stress but h_1 does not contain initial stress supports more to V_i (i = 1…6) than as compared to the case when h_1 contains initial stress but h_2 does not contain initial stress.

The current study for wave propagation is significant for geophysics, seismologists and metallurgy and is also beneficial in sound system, signal processing, and wireless communication.

Appendix A

$$h_{11}=1,\ h_{12}=2\underline{\mu}\sin\sin\theta_0\frac{\sqrt{1-s_{21}^2\theta_0}}{D_1 s_{31}},$$

$$h_{13}=-\frac{(\bar{\bar{\lambda}}+\bar{\bar{h}})+2\bar{\bar{\mu}}(1-S_{11}'^2)\sin\sin\theta_0}{D_1 S_{11}'^2},\ h_{14}=\frac{2\bar{\bar{\mu}}\sin\sin\theta_0\sqrt{1-S_{41}'^2\theta_0}}{D_1 S_{41}'^2},$$

$$h_{21}=-1,\ h_{22}=\frac{a}{\underline{\mu}}s_{21}^2 l_2^2,\ h_{23}=\frac{\mu}{\underline{\mu}}S_{11}'^2,\ h_{24}=\frac{a}{\underline{\mu}}s_{41}'^2 l_2'^2,\ h_{31}=1,$$

$$h_{32}=\frac{-\sin\sin 2\theta_0\left[\sin\sin\theta_0+\sqrt{1-s_{21}^2\sin\sin\theta_0}\right]}{s_{21}^3},$$

$$h_{33}=\frac{\sin\sin 2\theta_0\left[\sin\sin\theta_0+\sqrt{1-S_{11}'^2\theta_0}\right]}{S_{11}'^3},\ h_{34}=\frac{2\theta_0\left[\sin\sin\theta_0+\sqrt{1-S_{41}'^2\theta_0}\right]}{S_{41}'^3},$$

$$h_{41}=\cos\cos\theta_0,\ h_{42}=\sin\sin\theta_0,\ h_{43}=\frac{\sqrt{1-S_{11}'^2\theta_0}}{S_{11}^2},\ h_{44}=-\sin\sin\theta_0,$$

$$h_{51}=\sin\sin\theta_0,\ h_{52}=\frac{\sqrt{1-s_{21}'^2\theta_0}}{s_{21}^2},\ h_{53}=-\sin\sin\theta_0,\ h_{54}=\frac{\sqrt{1-S_{21}'^2\theta_0}}{S_{21}^2},$$

where: $s_{21} = s_2/s_1$; $s_{r1}' = s_r'/s_1$ (r = 1, 2); $S_{11}' = s_{11}'$; $S_{41}' = s_{21}'$; $D_1 = [(\underline{\lambda} + \underline{h}) + 2\mu\theta_2]$.

$Z_1 = 1$, $Z_2 = -1$, $Z_3 = \sin\sin 2\theta_0(\sin\sin\theta_0 + \cos\cos\theta_0)$, $Z_4 = \sin\sin\theta_0$.

Appendix B

$$U_{11}=\frac{(\underline{\lambda}+\underline{h})+2\underline{\mu}(1-s_{12}^3)\theta_0}{D_1 s_{12}^2},\ U_{12}=1,\ U_{13}=-\frac{(\bar{\bar{\lambda}}+\bar{\bar{h}})+2\bar{\bar{\mu}}(1-S_{12}'^2)\theta_0}{D_1 s_{12}'^2},$$

$$U_{14}=2\bar{\bar{\mu}}\frac{\sin\sin\theta_0\sqrt{1-S_{42}'^2\theta_0}}{D_1 S_{42}'^2},\ U_{21}=s_{12}^2,\ U_{22}=-1,\ U_{23}=\frac{\bar{\bar{\mu}}}{\underline{\mu}}s_{12}'^2,$$

$$U_{24}=\frac{\bar{\bar{a}}}{\underline{\mu}}S_{42}'^2 t_2'^2,\ U_{31}=\frac{\sin\sin 2\theta_0\left[\sin\sin\theta_0+\sqrt{1-s_{12}^2\theta_0}\right]}{s_{12}^3},$$

$$U_{32}=\frac{2\theta_0\left[\sin\sin\theta_0+\sqrt{1-s_{22}^2\theta_0}\right]}{s_{22}^3},\ U_{33}=\frac{\sin\sin 2\theta_0\left[\sin\sin\theta_0+\sqrt{1-S_{12}'^2\theta_0}\right]}{s_{12}'^3},$$

$$U_{34}=\frac{2\theta_0\left[\sin\sin\theta_0+\sqrt{1-S_{42}'^2\theta_0}\right]}{S_{42}'^3},\ U_{41}=\frac{\sqrt{1-s_{12}^2\theta_0}}{s_{12}^2},\ U_{42}=1,$$

$$U_{43}=\frac{\sqrt{1-S_{12}'^{2}\theta_0}}{s_{12}'^{2}},\ U_{44}=-\sin\sin\theta_0,\ U_{51}=\sin\sin\theta_0,\ U_{52}=-1$$

$$U_{53}=-\sin\sin\theta_0,\ U_{54}=\frac{\sqrt{1-s_{42}'^{2}\theta_0}}{s_{42}'^{2}},$$

where: $s_{12} = s_1/s_2$; $s_{r2}' = s_r'/s_2$ (r = 1, 2); $S_{42}' = s_{12}'$; $D_2 = 2\mu \cos\cos\theta_0 \sin\sin\theta_0$.

$$W_1=1,\ W_2=-1,\ W_3=\sin\sin 2\theta_0(\sin\sin\theta_0+\cos\cos\theta_0),$$

$$W_4=-\sin\sin\theta_0,\ W_5=\cos\cos\theta_0 .$$

REFERENCES

1. Voigt, W., *Theoretische Studien über die Elastizitätsverhältnisse der Krystalle*, Band 34, Abhandlungen der Mathematischen Classe der Königlichen Gesellschaft der Wissenschaften zu Göttingen, Dieterichsche Verlags-Buchhandlung, 1887: 3-100. (*Theoretical studies on the elasticity conditions of crystals*, Vol. 34, Treatises of the Mathematical Class of the Royal Society of Sciences in Göttingen, *in German*).
2. Cosserat, E., Cosserat, F., Théorie des Corps déformables, Librairie Scientifique A. Herman et. Fils, Paris, 1909, p.230. (*Theory of Deformable Bodies*, in French).
3. Toupin, R.A. (1962), *Elastic materials with couple-stresses*, Arch. Rational Mech. Anal. 11(1): 385-414. doi: 10.1007/BF00253945
4. Mindlin, R.D., Tiersten, H.F. (1962), *Effects of couple-stresses in linear elasticity*, Arch. Rational Mech. Anal. 11: 415-448. doi: 10.1007/BF00253946
5. Anthoine, A. (2000), *Effect of couple-stresses on the elastic bending of beams*, Int. J Solids Struct. 37(7): 1003-1018. doi: 10.1016/S0020-7683(98)00283-2
6. Lubarda, V.A., Markenscoff, X. (2000), *Conservation integrals in couple stress elasticity*, J Mech. Phys, Solids, 48(3): 553-564. doi: 10.1016/S0022-5096(99)00039-3
7. Lubarda, V.A. (2003), *Circular inclusions in anti-plane strain couple stress elasticity*, Int. J Solids Struct. 40(15): 3827-3851. doi: 10.1016/S0020-7683(03)00227-0
8. Gourgiotis, P.A., Georgiadis, H.G. (2008), *An approach based on distributed dislocations and disclinations for crack problems in couple-stress elasticity*, Int. J Solids Struct. 45(21): 5521-5539. doi: 10.1016/j.ijsolstr.2008.05.012
9. Güven, U. (2011), *The investigation of the nonlocal longitudinal stress waves with modified couple stress theory*, Acta Mech. 221(3-4): 321-325. doi: 10.1007/s00707-011-0500-4
10. Eringen, A.C. (1966), *Linear theory of micropolar elasticity*, J Math. Mech. 15(6): 909-923.
11. Sahrawat, R.K., Poonam (2021), *Reflection-refraction coefficients and energy ratios in couple stress micropolar thermoviscous elastic solid*, Int. J Appl. Mech. Eng. 26(2): 47-69. doi: 10.2478/ijame-2021-0019
12. Poonam, Sahrawat, R.K., Kumar, K. (2021), *Plane wave propagation and fundamental solution in non-local couple stress micropolar thermoelastic solid medium with voids*, Waves Random Complex Media, 34(2): 879-914. doi: 10.1080/17455030.2021.192131
13. Sahrawat, R.K., Kumar, K., Poonam, Rani, S. (2023), *Reflection and refraction phenomenon of waves at the interface of two non-local couple stress micropolar thermoelastic solid half-spaces*, Mech. Solids, 58: 216-244. doi: 10.3103/S0025654422600891
14. Biot, M.A. (1940), *The influence of initial stress on elastic waves*, J Appl. Phys. 11(8): 522-530. doi: 10.1063/1.1712807
15. Tochhawng, L., Singh, S.S. (2020), *Effect of initial stresses on the elastic waves in transversely isotropic thermoelastic materials*, Eng. Reports, 2(1): e12104. doi: 10.1002/eng2.12104
16. Saha, S., Singh, A.K., Chattopadhyay, A. (2020), *Analysis of reflection and refraction of plane waves at the interface of two functionally graded incompressible monoclinic media under initial stress and gravity*, Eur. Phys. J Plus, 135: art. no. 173. doi: 10.1140/epjp/s13360-020-00189-y
17. Goyal, R., Kumar, S. (2021), *Estimating the effects of imperfect bonding and size-dependency on Love-type wave propagation in functionally graded orthotropic material under the influence of initial stress*, Mech. Mater. 155: 103772. doi: 10.1016/j.mechmat.2021.103772
18. Poonam, Sahrawat, R.K., Kumar, K., Arti (2021), *Plane wave propagation in functionally graded isotropic couple stress thermoelastic solid media under initial stress and gravity*, Eur. Phys. J Plus, 136: art no.114. doi: 10.1140/epjp/s13360-021-01097-5
19. Wang, X., Chen, Y., Yu, J., et al. (2023), *Energy distribution of plane waves in functionally graded nonlocal integral thermo-electro-elastic nanoplates in liquid*, Mech. Adv. Mater. Struct. 31(28): 10098-10111. doi: 10.1080/15376494.2023.2284860
20. Poonam, Malik, S., Antil, A., et al. (2023), *Impact of initial stress on wave propagation in exponentially graded isotropic nonlocal generalized thermoelastic solid medium*, Mech. Solids, 58: 939-960. doi: 10.3103/S0025654423600320